

THE AYLI DAĞ OPHIOLITE SEQUENCE (CENTRAL-NORTHERN TURKEY): A FRAGMENT OF MIDDLE JURASSIC OCEANIC LITHOSPHERE WITHIN THE INTRA-PONTIDE SUTURE ZONE

M. Cemal Göncüoğlu*, Michele Marroni**^{o,✉}, Kaan Sayit***, U. Kagan Tekin^o, Giuseppe Ottria^o
and Luca Pandolfi**^o, Alessandro Ellero^o

* Department of Geological Engineering, Middle East Technical University, Ankara, Turkey.

** Dipartimento di Scienze della Terra, Università di Pisa, Italy.

*** Department of Geological Sciences, San Diego State University, USA.

^o Istituto di Geoscienze e Georisorse, CNR, Pisa, Italy.

^o Department of Geological Engineering, Hacettepe University, Ankara, Turkey.

✉ Corresponding author: e-mail: marroni@dst.unipi.it

Keywords: Ophiolites, geochemistry, Radiolaria, back-arc basin, Intra-Pontide suture zone. Turkey.

ABSTRACT

The Ayli Dağ ophiolites occur as an independent tectonic unit within the Intra-Pontide suture zone, central-northern Turkey. They crop out, together with the other units of the Intra-Pontide suture zone, at the top of the Late Cretaceous-Middle Paleocene foredeep sediments of the Sakarya Terrane. The Ayli Dağ ophiolites sequence include in its lower part a mantle sequence consisting of not less than 2-3 km-thick peridotites, topped by 500-600 m-thick layered gabbros with alternating, dm- to m-thick layers of spinel-bearing dunites, melatroctolites, troctolites, ol-gabbros and leucogabbros. The gabbro sequence is overlain by a sheeted dyke complex, that shows a transition to 100-200 m-thick massive basaltic lava flows followed by 600-800 m-thick massive and pillow lavas and breccias alternating with ophiolite-bearing arenites and cherts.

Geochemical evaluation of the mafic lavas and dykes reveals three distinct chemical groups that reflect melt generation within an intra-oceanic subduction system. Among these, the first group shows island-arc tholeiite (IAT)-like features, showing very-depleted characteristics (very high Zr/Nb, low Zr/Y and Nb/Y) ratios coupled with light rare-earth (LREE)-depleted chondrite-normalized patterns. The second group is more akin to back-arc basin basalts (BABB); it displays normal mid-ocean ridge basalt (N-MORB)-like high-field strength element (HFSE) distribution except for depletion in Nb, and flat REE patterns. The third group is somewhat similar to the second one, displaying BABB-like characteristics, but it is more enriched in terms of absolute trace element abundances.

The radiolarian cherts sampled from the top of the pillow lavas yielded less-diverse but characteristic radiolarian assemblages indicating the middle Bathonian to early Callovian ages.

The Ayli Dağ Ophiolite is the first finding of back-arc type oceanic lithosphere in the Intra-Pontide suture zone. Together with previous data obtained from basalts in the mélange from the Intra-Pontide suture zone, this finding represents a proof that an intra-oceanic subduction within the Intra-Pontide oceanic basin occurred in the Middle Jurassic time.

INTRODUCTION

The number, locations as well as the evolution of the Tethyan oceanic seaways in SE Europe (e.g., Robertson and Dixon 1984; Robertson et al., 1991; Pamic et al., 1998; Robertson 2002; Bortolotti and Principi 2005; Schmid et al. 2008; Zelic et al., 2010; Chiari et al., 2011) and in the Mediterranean realm (e.g., Sengör and Yılmaz, 1981; Göncüoğlu et al., 1997; Okay and Tüysüz, 1999; Stampfli, 2000; Robertson, 2002; Bortolotti and Principi, 2005; Okay and Whitney, 2010; Varol et al., 2011) has been a matter of debate since long time. In this framework, the oceanic branches, opened during the Mesozoic and closed at the end of Cretaceous to generate a complex network of ophiolitic sutures within the Alpine orogenic belt (Fig. 1), are known as the Neotethyan oceans (e.g., Sengör, 1986). In Turkey, a general consensus has been achieved on the geodynamic interpretation of the main branches, namely the southern (Bitlis-Zagros) and the middle (Izmir-Ankara-Erzincan) ones, both represented by distinct ophiolite-bearing suture zones sandwiched between continental terranes (Fig. 1). The existence of the third one, known as the Intra-Pontide (IP) oceanic basin, located between the continental margins today represented by Sakarya (SK) and Istanbul-Zonguldak (IZ) terranes, is still a matter of debate (e.g., Kaya and Kozur, 1987; Kozur et al., 2000; Elmas and Yigitbas, 2001;

2005; Moix et al., 2008; Göncüoğlu et al., 2008, Bozkurt et al., 2012; Elmas, 2012). This is mainly due to the discontinuous occurrence of the oceanic rocks along the Intra-Pontide suture (IPS) zone, whose primary features are modified by the deformation related to an active transform fault, the North Anatolian Fault (NAF), running parallel to the belt. These oceanic rocks mainly occur as tectonic slices and/or slide blocks into the mélange along a narrow strip stretching from the Biga Peninsula at the Aegean coast (Cetmi Mélange, Beccalotto et al., 2005) towards E, following the S coast of the Sea of Marmara (Mudanya-Zeytindagi Mélange, Ulgen and Okay, 2010), Armutlu Peninsula (e.g., Kaya and Kozur, 1987; Göncüoğlu et al., 1987; Akbayram et al., 2012), Southern Bolu Massif (Arkotdağ Mélange, Tokay, 1973; Abant Complex, Yılmaz et al., 1982), W of Gerede (Göncüoğlu et al., 2008) and Bolu-Eskipazar Zone (Elmas et al., 1997; Yigitbas et al., 1999). In the W, the IPS zone is assumed to join with the Vardar Suture and in the E to be bounded by a transform fault (E Crimean Fault of Okay and Tüysüz, 1999) or alternatively continues through the Kargi Massif (Göncüoğlu et al., 1997).

In most of these areas, the IPS zone consists of an assemblage of ophiolite-bearing mélange and continental- and oceanic-derived units, showing different metamorphic imprints. The mélange includes up to a few hundred m-large slide blocks of limestones, arenites and metamorphic rocks,

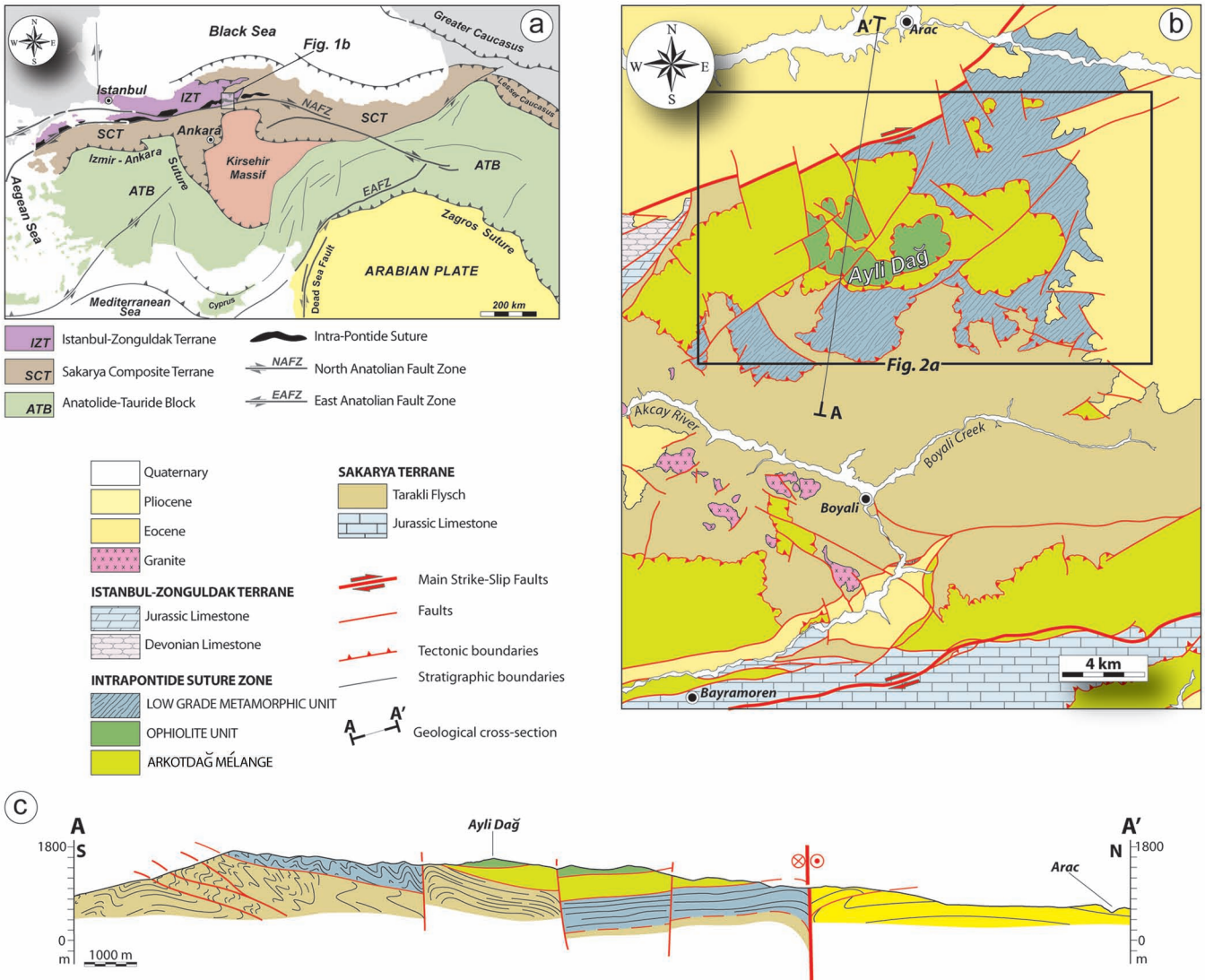


Fig. 1 - a: The major tectonic zones of Turkey with the main bodies of ophiolites (modified from Sengör and Yılmaz, 1981); b: geological sketch map of the Bayramoren-Arac area; c: related cross section.

but the most common lithologies are represented by serpentinized mantle rocks, gabbros, massive and pillow lavas and cherts. A limited number of studies (e.g., Robertson and Ustaömer, 2004; Göncüoğlu et al., 2008), mainly based on the geochemistry of the pillow lavas, indicate that the basalts are of oceanic origin, with MORB (Mid Ocean Ridge Basalts)- and OIB (Ocean Island Basalts)-type characteristics. The matrix of the mélangé has provided Late Cretaceous fossils (Kaya and Kozur, 1987; Göncüoğlu and Erendil, 1990; Beccaletto et al., 2005; Göncüoğlu et al., 2008). Based on this age data, Göncüoğlu et al. (2008) suggested that the closure of the IP oceanic basin was not realized before the Late Cretaceous.

In this study, we will report the occurrence of an ophiolite sequence on the eastern part of the IPS to the South of Arac in the Ayli Dağ area (Fig. 1). It differs from the previously described remnants of the IP oceanic basin in the west not only for its geochemical characteristics but also because it is represented by an almost complete ophiolite sequence, from mantle rocks to sedimentary cover. In this paper a complete set of geological, petrographical, geochemical and paleontological features of the Ayli Dağ ophiolites sequence are reported. These data may provide useful constraints for

the reconstruction of the geodynamic history of the IPS zone.

GEOLOGICAL SETTING OF AYLI DAĞ AREA

In the eastern Central Pontides, to the S of Kastamonu, the IPS zone consists of an imbricate stack of tectonic units consisting of metamorphic rocks, ophiolites and an ophiolite-bearing mélangé, with the latter reported as Arkotdağ Mélangé (Tokay, 1973). These units, bounded by low-angle E-W trending thrusts showing top-to-the-south sense of shear, are emplaced over the sedimentary cover of the SK terrane, whose top is represented by the foredeep deposits of the Tarakli Flysch of Late Cretaceous-Middle Paleocene age (Catanzariti et al., 2012). In turn, the IPS units are topped by a Klippen of the IZ terrane as recognized south of the Iğdir village, west of Ayli Dağ Mt. (Fig. 1).

The relationships among these IPS units are sealed by the Early Eocene deposits of Safranbolu-Karabük basin that widely crop out in the southern flank of the Ayli Dağ Mts. along the Arac valley. Thus, the development of the imbricate stack can be regarded as the result of pre-Eocene

tectonics leading to deformation of the IPS units and, subsequently, to their imbrication by multiple events of thrusting. Probably, in its original tectonic setting the continental units were located at the top of the ophiolite unit and the associated Arkotdağ Mélange. Additionally, the tectonics related to the North Anatolian Fault Zone, consisting of several events of transpression and transtension, strongly reworked since Miocene the structural setting of the imbricate stack of IPS zone. These events produced subvertical strike-slip faults and the related low-angle reverse faults that cut across the Eocene deposits as well as the boundaries of the different units of IPS zone.

The metamorphic unit in Ayli Dağ Mt. is represented by the Low Grade Metamorphic (LGM) Unit. The LGM Unit consists of a thick succession of actinolite-bearing metabasites, metacarbonates, metapelites, metarenites and metal-

idites cut by non-metamorphic basic dykes. It is characterized by a complex deformation history, consisting of four pre-Eocene phases, from D₁ to D₄, developed under retrograde P and T conditions. The D₁ and D₂ phases of LGM Unit were developed under blueschists to greenschists metamorphic facies conditions (Marroni et al., unpublished data), whereas the following phases are associated with very low-grade metamorphism.

The Arkotdağ Mélange is represented by a 1-2 km-thick succession of slide blocks, with different sizes and lithologies, enclosed in a sedimentary matrix consisting of shales, pebbly mudstones, pebbly sandstones and coarse-grained arenites. In the study area, the matrix includes a late Santonian nannofossil assemblage (Catanzariti et al., 2012). The slide blocks includes cherts ranging in age from Middle Triassic to Early Cretaceous, limestones and dolomitic lime-

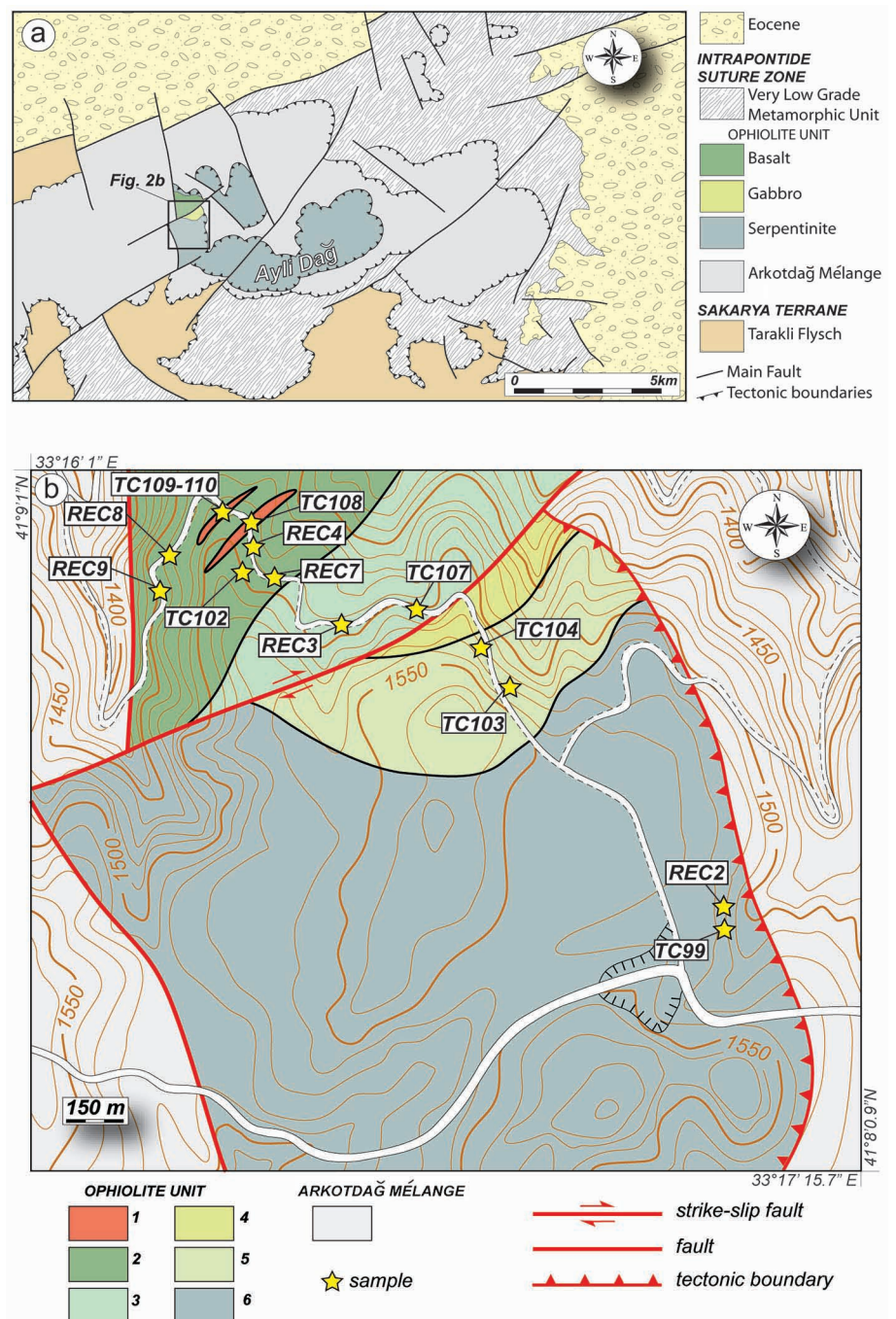


Fig. 2 - Geological sketch map of the Ayli Dağ area. 1- Cherts; 2- Pillow basalts and pillow breccia; 3- Sheeted dyke complex; 4- Gabbros; 5- Spinel-bearing dunites, melatroctolites and troctolites; 6- peridotites.

stones ranging in age from Triassic to Late Cretaceous, IAT (Island Arc Tholeiites) to BABB (Back-Arc Basin Basalts) basalts, gabbros, serpentinites and metamorphic rocks. In addition, slide blocks of a well-preserved Late Cretaceous succession consisting of cherty limestones, ophiolite-bearing arenites and mudstones has been found. The Arkotdağ Mélange is affected by a polyphase, even if localized, deformation, fully acquired at shallow structural levels with development of a very low-grade metamorphism.

THE AYLI DAĞ OPHIOLITE SEQUENCE

In the Ayli Dağ area, the ophiolite sequence was recently mapped in detail (Fig. 2). The Ayli Dağ ophiolites sequence crop out along the western flank of the Ayli Dağ Mt., just 3.5 km west of Siragözü Yayla, close the quarry of Kurtkayasi Hill (LAT41°8'46.66"N-LONG33°16'46.51"E - 1/25.000 scale Kastamonu F30c1 sheet).

The outcrops are crossed by the dirt road that starts from the Kurtkayasi quarry along the Siragözü-Munay Yayla main road and continues northward, towards the Arac valley. The studied sequence starts from the peridotites of the Kurtkayasi quarry and ends 3 km northwards.

The ophiolite sequence (Fig. 3a) includes a mantle section topped by an intrusive sequence whose uppermost levels are not recognized in the field due the occurrence of a WSW-ESE trending strike-slip fault. However, not less than 2-3 km-thick peridotites and 500-600 m-thick gabbros are exposed. In addition, about a 1-1.2 km-thick effusive sequence with a sheeted dyke complex showing a transition to massive and pillow-lavas. The basaltic flows are topped in turn by a thick sequence of pillow breccias, ophiolite-bearing arenites and cherts.

The mantle section consists of peridotites showing a foliation marked by aligned clinopyroxene minerals. Olivine, spinel and Fe-oxides can be also observed. Pyroxenite and dunite bands (Fig. 4a) are scarce and mainly located in the peridotites close to the base of the intrusive section. Rare rodingites, generally boudinaged, can be locally observed. Close to the Kurtkayasi Hill quarry a dolerite dyke cutting the peridotites has been found. The peridotites are affected by medium to low serpentinization degree with serpentinite minerals found in the groundmass of the peridotites or in mm-thick veins showing both isotropic and fibrous textures.

Above, at least a 400 m-thick sequence of layered gabbros crops out. This sequence includes alternating, dm- to m-thick layers of spinel-bearing dunites, melatroctolites and troctolites (Fig. 4b). Locally, cm-thick plagiogranite dykes cut at high angle the layered gabbros. Upwards, the troctolites show a transition in some tens of meters to gabbros. The isotropic ol-gabbros and leucogabbros (ca 150-200 m-thick) are characterized by both medium- and coarse-grained textures. Basalts characterized by porphyritic texture have been observed as dykes cutting the gabbros. The sequence is interrupted by the WSW-ESE trending fault that hampers any observation of the uppermost levels of intrusive complex.

To the north of this fault, a sheeted dyke complex occurs, characterized in its lower part by a network of dykes with scarce gabbroic screens. The sheeted dyke complex consists of a nearly 150 m-thick section of mutually intrusive dm-thick dykes with different color, texture and grain (Fig. 4c). The sheeted dyke complex shows a transition to a 100-200 m-thick massive lava flows characterized by basalts with

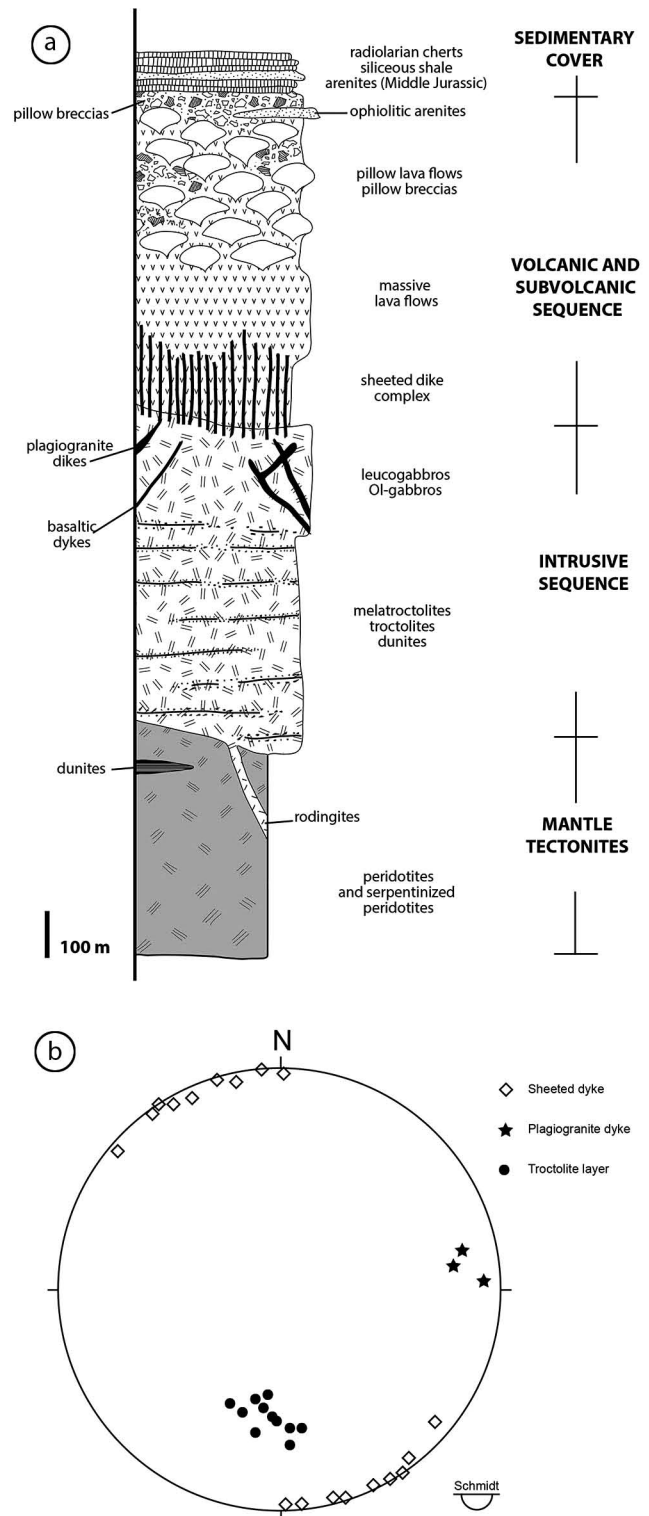


Fig. 3 - a: Stratigraphic log of the Ayli Dağ ophiolites sequence; b: stereographic net of attitude of gabbro layers, plagiogranite dykes and dykes from sheeted dyke complex.

well developed fine to medium grained holocrystalline texture. The relationship between the sheeted dyke complex and the massive lava flows is marked by lava sheets cut by scattered dykes. In turn, the massive lavas flows show a transition to pillow lava basalts showing a thickness of about 200-300 m. At the top, a 400-500 m-thick sequence of massive and pillow lavas (Fig. 4d) alternating with ophiolite-bearing arenites, siliceous mudstones and cherts occur.

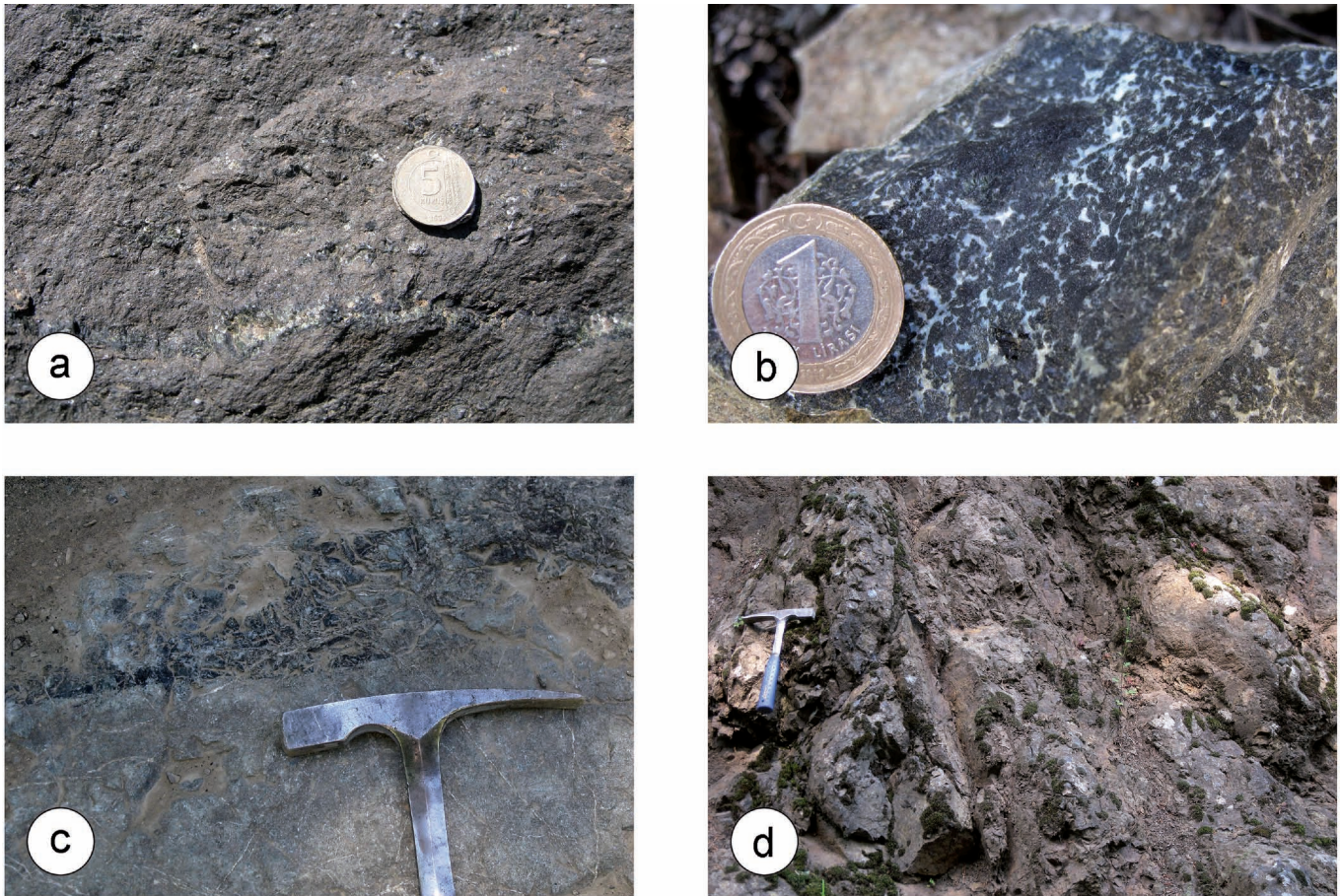


Fig. 4 - Field occurrence from Ayli Dağ ophiolites sequence: a- serpentinized peridotites; b- troctolites; c- contact between dykes in the sheeted dyke complex; d- pillow-lavas.

The cherts are represented by well stratified beds showing a thickness ranging from 10 to 30 cm. The arenite is thick-bedded to massive and mainly characterized by fragments of very altered basalt.

In the ophiolite sequence the lithological boundaries and the layering in the intrusive sequence show an attitude with about E-W strike and a dipping of 40-60° toward NW and NE. The plagiogranite dykes are characterized by N-S trending strike with vertical attitude. In turn, the sheeted dyke complex shows a NNW-SSE with subvertical attitude (Fig. 3b).

The ophiolite sequence is characterized by the complete lacking of orogenic-related ductile deformation and metamorphism. Probably, the deformations related to orogenic events are represented by brittle shear zones located at the boundaries of the ophiolite tectonic unit as well as the dipping of the layering in the intrusive sequence. However, the main deformation that affects the ophiolites consists of strike-slip faults showing both N-S and NE-SW strikes. These faults can be interpreted as belonging to antithetic system of the main fault that run south of Arac valley. This fault has been regarded as connected to the North Anatolian Fault (NAF) system.

PETROGRAPHY

Twenty two samples were taken from the different rock-units of the Ayli Dağ ophiolites sequence for petrographic

investigation. The peridotites are medium to coarse grained with anhedral granular texture (Fig. 5a). Olivines are variably serpentinized and strained. Pyroxenes are enstatites and include clinopyroxene lamellae. Chromite is the only opaque phase.

The sample REC-2 (Table 1) derives from a dolerite dyke cutting the peridotites. The dolerites show an equigranular, ophitic to subophitic, texture where the primary mineralogy consists of plagioclase and clinopyroxene, typically augite, with minor olivine, magnetite and ilmenite. However, the dolerites include also brownish magmatic hornblende, which is not observed in the basalts. Hornblende is largely replaced by actinolitic amphibole and chlorite. Epidote also appears in the dolerites as a secondary phase replacing plagioclase together with to sericite.

Troctolites are characterized by cumulate texture with olivine-dominant mineralogy. In these rocks, olivine is present as cumulus phase, while plagioclase, orthopyroxene and clinopyroxene are intercumulus phases (Fig. 5b). The ol-gabbros are characterized by a poikilitic texture with rounded olivine and pyroxene enclosed in plagioclase oikocrysts (Fig. 5c).

The sheeted dyke complex consists of basalts with different texture, from porphyric to hypocrySTALLINE including fine to coarse grained varieties. Chilled margins are widespread among the different dykes (Fig. 5d). The sample REC-3 (Table 1) is characterized by a porphyric texture with albite phenocrysts set in an holocrystalline groundmass with intersertal texture marked by plagioclase laths. Other samples

Table 1 - Chemical analyses of basalts (REC-2 to REC-9).

	Group 1		Group 2	Group 3				
	REC-2	REC-3	REC-9	REC-4	REC-5	REC-6	REC-7	REC-8
SiO ₂	48.38	50.24	46.79	48.00	50.46	46.26	46.06	49.14
Al ₂ O ₃	16.34	15.34	14.96	13.39	13.50	13.22	13.23	12.67
Fe ₂ O ₃	7.37	8.31	9.12	10.37	10.84	11.82	12.34	12.11
MgO	9.23	9.05	6.34	5.71	5.95	6.22	6.73	6.76
CaO	11.14	10.16	10.76	10.69	7.71	10.03	11.02	8.32
Na ₂ O	2.65	2.96	4.34	4.57	4.40	4.08	3.72	4.56
K ₂ O	0.22	0.22	0.03	0.23	0.28	0.13	0.04	0.15
TiO ₂	0.54	0.84	1.20	1.91	1.95	2.04	1.97	2.21
P ₂ O ₅	0.03	0.05	0.12	0.21	0.21	0.22	0.18	0.24
MnO	0.12	0.15	0.15	0.16	0.13	0.16	0.20	0.18
LOI	3.60	2.30	6.00	4.50	4.30	5.60	4.30	3.40
Sum	99.76	99.77	99.82	99.81	99.78	99.78	99.8	99.76
Sc	30	34	39	34	36	34	41	38
V	208	222	267	346	312	311	345	335
Cr	623	643	212	226	246	192	171	212
Ni	103.0	71.3	77.2	62.2	76.0	57.1	38.1	53.3
Co	36.2	37.2	37.9	35.2	39.4	37.1	42.6	38.0
Ba	17	13	18	11	47	24	5	7
Rb	4.0	2.9	0.4	1.7	7.7	3.8	0.7	1.3
Sr	414.2	214.0	107.6	145.8	210.0	151.1	91.2	145.9
U	b.d.	b.d.	1.3	0.3	0.3	0.3	0.1	0.3
Pb	0.2	0.2	0.9	0.8	1.6	0.9	0.8	0.7
Th	b.d.	b.d.	0.2	0.4	1.0	0.6	0.3	0.3
Hf	0.7	1.1	1.6	4.0	3.6	4.9	2.8	4.2
Nb	0.4	0.3	2.0	3.2	4.2	3.7	3.9	3.9
Ta	b.d.	b.d.	0.2	0.1	0.4	0.2	0.1	0.2
Zr	21.5	38.2	63.6	116.3	153.1	153.7	126.6	156.6
Y	15.8	21.9	23.7	41.9	42.4	47.3	44.1	49.1
La	0.70	1.10	4.50	6.60	8.00	7.10	4.70	5.60
Ce	1.90	3.60	10.60	17.80	20.30	19.40	14.30	17.50
Pr	0.41	0.71	1.60	2.97	3.06	3.01	2.31	2.86
Nd	1.60	4.60	9.50	16.00	18.20	17.20	15.40	14.40
Sm	1.15	1.81	2.64	4.87	4.95	4.98	4.61	4.99
Eu	0.43	0.72	1.11	1.62	1.63	1.65	1.51	1.68
Gd	2.00	3.03	3.72	6.00	6.86	7.07	6.23	7.16
Tb	0.39	0.57	0.69	1.27	1.18	1.30	1.21	1.35
Dy	2.72	3.50	3.71	7.01	7.00	8.44	8.14	8.05
Ho	0.59	0.86	0.94	1.75	1.71	1.78	1.63	1.87
Er	1.77	2.29	2.60	4.83	4.76	5.34	4.49	5.10
Tm	0.30	0.38	0.38	0.69	0.68	0.75	0.72	0.79
Yb	1.70	2.06	1.97	4.40	4.41	4.74	4.54	4.71
Lu	0.28	0.36	0.35	0.67	0.65	0.77	0.59	0.71

b.d.- below detection limit.

from sheeted dyke complex are characterized by holocrystalline subophitic coarse to medium grained texture with plagioclase, pyroxene and olivine as main components.

Sample REC-4 to 9 (Table 1) have been collected in both massive and pillowed flow basalts, with the latter closely associated with pillow breccias. The pillow structures are in the upright position so that the range of these five samples represents the magmato-stratigraphic order.

The samples from the crustal section of the Ayli Dağ ophiolites include different types of basalts that are all variably altered. Basaltic types are hypocrySTALLINE to holocrystalline, and mostly show porphyric textures. Glass, however, is now devitrified and replaced by secondary phases, such as chlorite and clay minerals. Some porphyric samples are characterized by relatively large phenocrysts attaining size of ~ 0.5-0.7 cm (Fig. 5e). Basalts reflect a primary

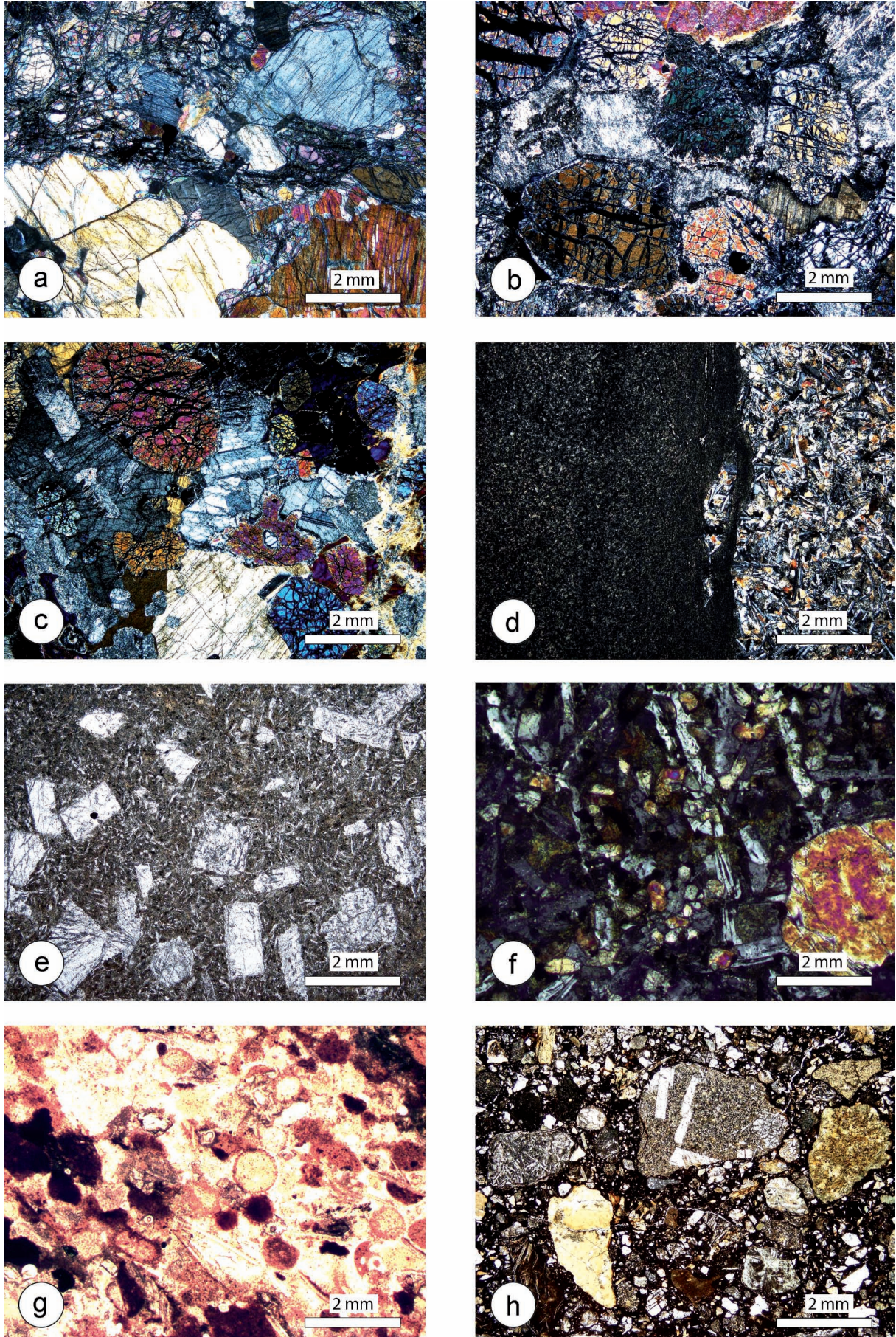


Fig. 5 - Microscopic features of Ayli Dağ ophiolites: a- peridotite; b- troctolite; c- ol-gabbro; d- chilled margin between dykes from sheeted dyke complex; e- phenocrysts of plagioclase and clinopyroxene from pillow lava basalts; f- idiomorphic augite phenocrysts from the pillow lava basalts; g- siliceous mudstone with radiolarian tracks, reworked microfossils, micritic limestone and basalt clasts; h- ophiolite-bearing arenites.

mineral assemblage composed of plagioclase + clinopyroxene \pm olivine + opaque minerals. Where found, olivine is observed to be partially or completely replaced by secondary minerals including serpentine and chlorite (Fig. 5f). Plagioclase is, in most cases, altered to sericite, calcite and chlorite. Clinopyroxene is relatively fresh compared to olivine and plagioclase. In some cases, however, it is altered to actinolite, chlorite and calcite. Glomeroporphyric clusters of clinopyroxene are also common.

The sedimentary cover of the pillow basalts are characterized by radiolarian cherts, siliceous mudstones (Fig. 5g) and ophiolite-bearing arenites (Fig. 5h). The latter can be classified as quartz-free litharenite where the angular fragments were derived totally from an ophiolite sequence. The most common fragments are represented by volcanic and subvolcanic rocks consisting of dolerites and aphyric to porphyritic basalts. The other fragments of crustal rocks are gabbros and plagiogranites.

GEOCHEMICAL FEATURES OF THE VOLCANIC ROCKS

A total of 8 samples of basalts were analyzed for major and trace elements in the ACME Labs (Canada). The relatively large range in loss on ignition (LOI) values (2.3-6.0 wt%) suggests that the samples have been variably affected by post-magmatic processes (e.g., alteration, oceanic meta-

morphism). These conditions may lead to the selective mobility of some elements, such as Rb, Sr, Na and K (e.g., Staudigel et al., 1996). Therefore, in our petrogenetic interpretation, we use the elements that are thought to be relatively immobile during alteration/metamorphism, such as Th, high-field strength elements (HFSE) and rare-earth elements (REE) (e.g., Ludden et al., 1982; Arculus et al., 1999). The stable behaviors of these elements are demonstrated by the coherent patterns on the trace element and REE variation plots (Fig. 6).

The analyzed samples display variable MgO contents (6.0-9.6 wt%, calculated on volatile-free basis), suggesting that some of the sample compositions may reflect modification by fractional crystallization. All samples have subalkaline composition, as reflected by variable, but low Nb/Y ratios (0.01-0.10) (Fig. 7). On the basis of trace element systematics, three chemical groups are identified.

The first group (Group 1) displays depleted characteristics, showing apparent depletion in the most incompatible elements relative to normal N-MORB (Normal-Mid Ocean Ridge Basalt) (Fig. 6). The second group (Group 2), represented by a single sample (REC-9) in the dataset, is characterized by mainly N-MORB-like HFSE distribution coupled with slight depletion in Nb (Fig. 6). The third group (Group 3) is somewhat similar to Group 2, but more enriched than the latter. Group 3 samples also show negative Nb anomalies and they are largely characterized by HFSE patterns sub-parallel to that of N-MORB (Fig. 6).

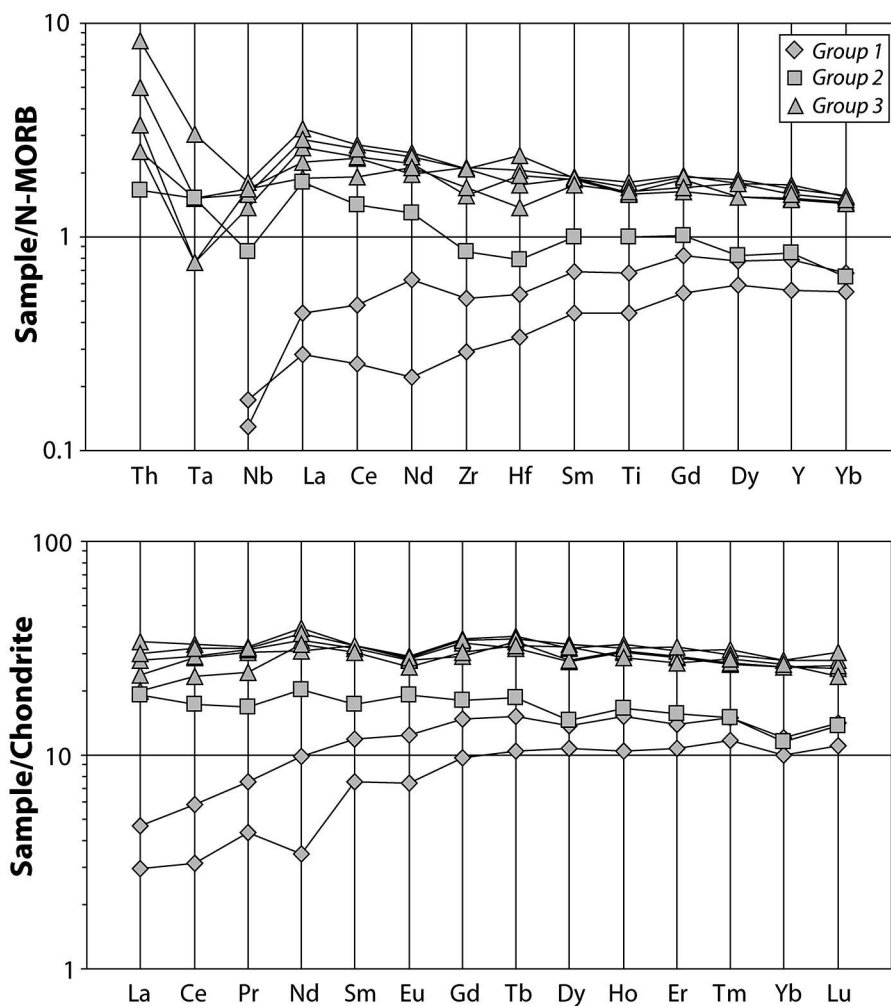


Fig. 6 - Incompatible element and REE patterns of the Ayli Dağ basalts. Normalization values from Sun and McDonough (1989).

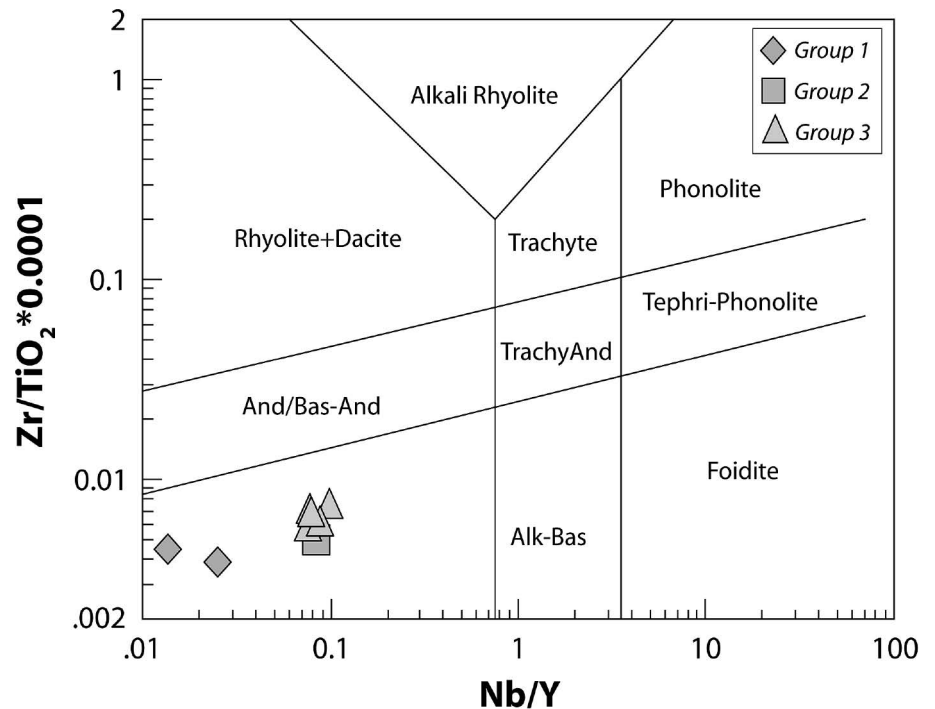


Fig. 7 - Chemical classification of the Ayli Dağ basalts on the basis of immobile elements. According to Winchester and Floyd (1977) diagram revised by Pearce (1996).

Group 1 samples show very high Zr/Nb ratios ranging between 53.8 -127.3. Groups 2 and 3 samples display somewhat similar Zr/Nb ratios to each other (31.8 and 32.5-41.5, respectively); however they both show lower Zr/Nb values than those of Group 1. In terms of Nb/Y ratio, Group 1 displays the lowest values, between 0.01-0.03, whereas the other groups show higher ratios, ranging between 0.08-0.10. Group 1 samples are also distinct with regard to their low TiO₂ contents which ranges between 0.6-0.9 (wt%) (calculated on volatile-free basis).

The comparison among the three groups indicates that the Group 2, with its TiO₂ content of 1.3 (wt%), shows intermediate features between Group 1 and Group 3. Group 3 suite, on the other hand, displays the highest ratios that vary between 2.0-2.3. On chondrite-normalized REE plots, Group 1 suite is characterized by light REE (LREE)-depleted patterns, whereas Groups 2 and 3 show relatively flat REE patterns. Although the latter two groups display similar REE variations to each other, Group 3 suite differs from Group 2 in having more enriched absolute abundances. N-MORBs are generally thought to be generated in response to decompression melting of asthenospheric upper mantle or depleted MORB mantle (DMM) (e.g., Zindler and Hart, 1986; McKenzie and O'Nions, 1991). This depleted mantle reservoir is characterized by high Zr/Nb ratio (34.2; Workman and Hart, 2005). N-MORBs, in general, also show high Zr/Nb ratios (31.8; Sun and McDonough, 1989), suggesting that they are medium/high degree melt products of DMM.

Group 1 suite of the Ayli Dağ ophiolites display Zr/Nb ratios (53.8-127.3) even higher than the average N-MORB. This very-depleted nature of Group 1 samples is also suggested by Zr/Y and Nb/Y ratios (1.36-1.74, 0.01-0.03, respectively) which are apparently lower than those of N-MORB (2.64, 0.08, respectively; Sun and McDonough, 1989) (Fig. 8). Furthermore, Group 1 samples display N-MORB-normalized trace element patterns showing a gradual depletion towards the more incompatible elements. Such geochemical signatures cannot be obtained simply by melting a DMM-type mantle. Instead they require a previous

melt extraction from a DMM-type mantle source (e.g., Pearce and Parkinson, 1993). The highly depleted nature of Group 1 suite, therefore, may reflect melt generation from an already depleted mantle source.

In contrast to Group 1, the lower Zr/Nb and Y/Nb ratios of Group 2 and 3 suites may suggest relatively more fertile mantle source. The N-MORB-like trace element characteristics of the latter groups indicate their derivation from a DMM-type source. The relatively enriched characters of Group 2 and 3 suites are also evidenced by the chondrite-normalized REE patterns. These groups display apparently higher LREE/MREE ratios ([La/Sm]_N = 0.7-1.1) compared to Group 1 which is LREE depleted ([La/Sm]_N = 0.4). It must be noted that Group 2 and Group 3 suites reflect somewhat similar trace element ratios and patterns; however Group 3 samples have higher absolute abundances relative to Group 2.

This may suggest that although both groups may have derived from mantle sources reflecting somewhat similar trace element ratios, the source of Group 3 appears to be more enriched in terms of absolute abundances. The similar MgO contents of the Group 2 and 3 samples suggest that the relative enrichment of Group 3 is not due to fractional crystallization.

Magma generated in subduction zones show diverse trace element characteristics, such as negative Nb anomaly and enrichment in large-ion lithophile elements (LILE) and LREE relative to HFSE and HREE (e.g., Pearce and Peate, 1995). These distinct elemental signatures are generally attributed to the modification of mantle wedge by slab-derived components (e.g., Ellam and Hawkesworth, 1988; McCullough and Gamble, 1991).

Group 2 and 3 samples from Ayli Dağ ophiolites sequence show depletion in Nb, which is indicated by high Th/Nb and La/Nb ratios (0.08-0.24 and 1.21-2.25, respectively) relative to N-MORB (0.05 and 1.07, respectively; Sun and McDonough, 1989). These features may indicate a subduction-related contribution to the mantle source of samples from Ayli Dağ ophiolites sequence. In this regard, the

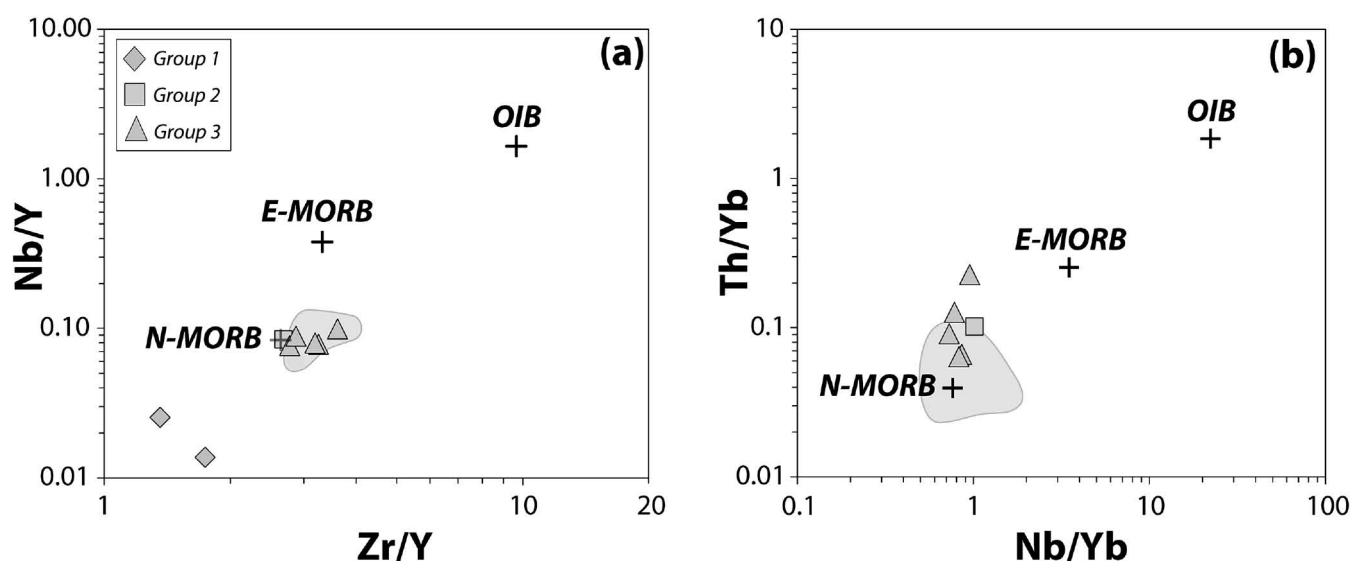


Fig. 8 - Ratio-ratio plots of the samples from the Ayli Dağ basalts. Data from Göncüoğlu et al. (2008) are reported for comparison (grey field). Average N-MORB, E-MORB and OIB values are from Sun and McDonough (1989).

use of Th/Yb and Nb/Yb pairs can be useful to detect the contribution from subduction component and the level of enrichment of the mantle source (Pearce, 1983; Pearce and Peate, 1995). Nb and Yb are regarded as subduction-immobile elements. In contrast, Th is subduction-mobile. Thus, subduction-related contributions would cause Th/Yb ratios to be displaced from the MORB array. In the plot of Nb/Yb vs Th/Yb, Group 2 and 3 suites deviate from the MORB array, suggesting that the mantle sources of these groups have been modified by subduction component.

TECTONO-MAGMATIC INTERPRETATION OF THE VOLCANIC ROCKS

Overall trace element systematics suggests that the melt generation of the Ayli Dağ ophiolites have probably occurred in an intra-oceanic subduction system. Although we cannot make any evaluation based on Th for the Group 1 suite, which is below detection limit, we think that this group has also formed in a subduction-related setting. Group 1 samples display depleted geochemical signatures, similar to island-arc tholeiites (IAT). Highly depleted melts, which reflect generation from a formerly depleted mantle, are frequently observed in island-arc magmas generated above intra-oceanic subduction zones (e.g., Elliott et al., 1997; Peate et al., 1997). This kind of melts is also commonly observed in Jurassic ophiolites from the Mediterranean area (e.g., Bortolotti et al., 2008; Saccani et al., 2008a; 2008b). This phenomenon is attributed to the previous melt extraction that took place in the back-arc region and subsequent flow of this pre-depleted mantle into the mantle wedge (e.g., Woodhead et al., 1993). Another explanation of this phenomenon implies that previously-depleted mantle, residual from MORB-melt extraction, forms the SSZ wedge and re-starts to melt once subduction is established. Examples of this case are reported from many peri-Mediterranean ophiolites (e.g., Saccani et al., 2008a; Bortolotti et al., 2012). The depleted characteristics of the IAT-type lavas are also demonstrated by Ti/V ratios which are generally lower than those of MORBs and BABBs (Sher-

vais, 1982; Woodhead et al., 1993). The relatively low Ti/V ratios of Group 1 samples, which range between 16.2 - 23.3, reinforce the idea that Group 1 suite reflects IAT-type characteristics. Group 1 samples also display relatively high La/Nb ratios (1.8-3.7) compared to N-MORBs (1.1; Sun and McDonough, 1989), which may constitute further support for the IAT-like nature of Group 1.

In contrast to Group 1, Group 2 and 3 samples are more akin to BABB-type magmas produced in oceanic back-arc basins (e.g., Gribble et al., 1998; Fretzdorff et al., 2002). This is especially evidenced by the intermediate characters of these groups between IAT and N-MORB (e.g., Gribble et al., 1998; Woodhead et al., 1998; Leat et al., 2004). Moreover, it is interesting to note that the geochemical characteristics of the Ayli Dağ BABBs are very similar to those of the BABBs from the Guevgueli Complex (Saccani et al., 2008c). In particular, they share flat chondrite normalized REE patterns, the same extent of Th enrichment (from 2 to 9 times N-MORB) and no or very little Nb depletion with respect to N-MORB, coupled with a little, but significant, Nb depletion with respect to Ti, Y, Yb. Group 2 and 3 suites reflect involvement of subduction component in their genesis, which are typically observed in arc-related magmas. However, Group 2 and 3 suites display Ti/V ratios (28.7-41.7) and HFSE systematics (except Nb-Ta) relatively similar to those of N-MORBs (Shervais 1982; Sun and McDonough, 1989), which suggest that these groups have been derived from a DMM-type mantle source rather than a pre-depleted mantle wedge. Compared to IATs, BABBs are generally of more enriched chemistry, as reflected by higher Ti/V and lower Zr/Nb (Shervais, 1982; Pearce et al., 1995; Fretzdorff et al., 2002). Thus, regarding Group 2 and 3 suites, these features seem to be more appropriate for a back-arc basin origin rather than an island-arc setting. The flat REE patterns of these groups further support this idea (e.g., Gribble et al., 1996; Sinton et al., 2003). These features fit with the presence of troctolites, that have also been reported from fossils examples of back-arc basins as well as from island-arcs from Pacific area (e.g., Hawkins and Evans 1983; Ichiyama and Ishiwatari, 1994), from North America (e.g., Lissenberg et al., 2005),

from Caribbean area (e.g., Tollan et al., 2011) and also from the Dinaric-Hellenic belt (Bortolotti et al., 2012). It is also noteworthy in this context that the Ayli Dağ BABB-type ophiolites share similar characteristics with those from the Guevueli Complex (Saccani et al., 2008c).

DATING OF RADIOLARIAN ASSEMBLAGES

Only two samples (11-TC-108 and 11-TC-109) from the sedimentary cover of the pillow basalts at Kurtkayasi Hill (Fig. 2) to the NW of Gölcük Yaylasi (LAT 41° 8'56.88"N-LONG 33°16'21.17"E - 1/25.000 scale Kastamonu F30c1 sheet) yielded less-diverse but abundant radiolarian assemblages (Fig. 9).

The collected chert samples have been etched by using diluted HF acid following the method suggested by Dumitrica (1970) and Pessagno and Newport (1972). All radiolarians obtained from these samples (see Plate 1) are stored at Paleontology Laboratory of the Geological Engineering Department, Hacettepe University, Ankara (Turkey).

These two assemblages are less-diverse and very similar to each other. They include characteristic taxa from Middle to Upper Jurassic time interval (Fig. 9). Although some of the taxa (e.g., *Transhuum brevicostatum* gr. (Ozoldova) and *Unuma gordus* Hull) in the sample 11-TC-108 have longer ranges (Ozoldova, 1975; Chiari et al., 2012), two well-known taxa define the age of the sample. *Spongocapsula palmerae* Pessagno first appears at middle Bathonian and disappears at the latest Tithonian (Pessagno, 1977; Pessagno et al., 1993; Baumgartner et al., 1995) while *Eucyrtidellum semifactum* Nagai and Mizutani has shorter range (latest Bajocian to top of early Callovian) (Nagai and Mizutani, 1990; Ozoldova, 1998; Baumgartner et al., 1995). Based on the co-occurrence of these taxa, the age of the sample 11-TC-108 is middle Bathonian-early Callovian corresponding to UAZ 6-7 by Baumgartner et al. (1995).

Radiolarian assemblage of the sample 11-TC-109 includes some long ranging taxa (Fig. 9). However, taking into the consideration of the first occurrence datum of *Spongocapsula palmerae* Pessagno (Pessagno, 1977; Pessagno et al., 1993; Baumgartner et al., 1995) and last appearance datum of *Stichomitra (?) takanoensis* Aita (Aita, 1987; Baumgartner et al., 1995), middle Bathonian to early Callovian age corresponding to UAZ 6-7 by Baumgartner et al. (1995) can be assigned to this sample.

Radiolarian assemblages of these two samples from NW Turkey are less-diverse compared with the radiolarian assemblages determined from the covalent strata in Turkey (Bragin et al., 2002; Tüysüz and Tekin, 2007; Tekin and Göncüoğlu, 2009) but include rather well-known taxa compared with assemblages from Tethyan and circum-Pacific belts.

GEODYNAMIC IMPLICATIONS

As previously reported, the existence of an IP oceanic basin is still matter of debate. Some authors (e.g., Elmas and Yigitbas, 2001; Moix et al., 2008; Bozkurt et al., 2012) deny the occurrence of ophiolites derived from an oceanic area located between the SK and IZ continental margins. Most of these authors (e.g., Moix et al., 2008) reached this conclusion simply because no reliable data are available for the magmatic rocks of the IPS zone.

SAMPLES		11-TC-108	11-TC-109			
AGE	TAXA	Zones by Baumgartner et al. (1995)	<i>Transhuum brevicostatum</i> gr. (Ozoldova) <i>Spongocapsula palmerae</i> Pessagno <i>Unuma gordus</i> Hull <i>Eucyrtidellum semifactum</i> Nagai and Mizutani <i>Spongocapsula palmerae</i> Pessagno <i>Unuma gordus</i> Hull <i>Stichomitra (?) takanoensis</i> Aita <i>Eucyrtidellum unumaense pustulatum</i> Baumgartner			
				BAJOCIAN		
				E M		
				L		
				BATHONIAN		
				E M		
				L		
				CALLOVIAN		
				E M		
				L		
				OXFORDIAN		
				E M		
				L		
KIMMERIDGIAN						
E						
L						
TITHONIAN						
E						
L						
	13					
	12					
	11					
	10					
	9					
	8					
	7					
	6					
	5					
	4					
	3					

Fig. 9 - Stratigraphic ranges of radiolarian taxa obtained from samples 11-TC-108 and 11-TC-109 from the cover of the pillow lavas of the Ayli Dağ ophiolites. Grey shaded area shows the supposed age of assemblages.

This paper provides, for the first time, the evidence of an almost complete ophiolite sequence preserved as a tectonic unit in the IPS zone. This ophiolite sequence represents a fragment of a back-arc oceanic lithosphere covered by cherts of middle Bathonian-early Callovian age (Middle Jurassic). This finding, as well as the occurrences into the Arkotdağ Mélange of numerous slide blocks of peridotites, gabbros and radiolarian cherts associated with oceanic

basalts, suggests that numerous remnants of an oceanic basin are preserved within the IPS zone (Marroni et al., unpublished data). This picture is confirmed by Göncüoğlu et al. (2008) that have described in the Arkotdağ Mélange from Bolu area a slide block of massive and pillow lavas that includes intra-pillow radiolarites and mudstones of Kimmeridgian to early Tithonian age. Geochemical data from these pillow basalts suggest their origin in a MOR setting characterized by a heterogeneous mantle modified by an earlier subduction.

All these evidences are against the scenarios disregarding the presence of the IP ocean (e.g., Elmas and Yigitbas, 2001; Moix et al., 2008; Bozkurt et al., 2012). The same conclusions are recently proposed by Elmas (2012) who also acknowledges the existence of the IP ocean basin.

Furthermore, the idea of Elmas and Yigitbas (2001; 2005), who proposed that the ophiolitic assemblages found within the IPS are actually remnants of the Izmir-Ankara Ocean emplaced by strike-slip tectonics between the SK and IZ terranes, is not consistent with the structural evidences from the study area. In this area the units from IPS zone are sandwiched between the SK and IZ terranes and bounded by low-angle, east-west trending thrust (Fig. 1) everywhere characterized by top-to-the-south sense of shear. The relationships among the units from IPS zone are sealed by Eocene deposits, as observed in the Arac area. This occurrence clearly indicates that the relationships between the IPS units and the SK and IZ terranes are acquired before the development of the NAF system, whose inception is regarded as Miocene in age. In addition, the features of the thrusts that bounded the IPS units, as their low-angle attitude or their same sense of shear, hamper their interpretation as related to a strike-slip tectonics.

In the light of our data, the existence of an oceanic basin, whose remnants are preserved as tectonic unit and slide blocks into the mélange of IPS zone, can now regarded as confirmed.

It is important to outline that the fundamental informations for a complete reconstruction of the geological history of the IPS zone are still lacking. The age of the opening of the oceanic basin(s) or the geodynamic mechanism of closure, remain open questions. In the same way, the features of the architecture of the IP basin, as, for instance, the occurrence of two co-existing MOR and SSZ oceanic basins separated by continental blocks or, in contrast, the existence of a large, single oceanic basin where an intra-oceanic subduction and an arc-back arc pair were active, cannot be reconstructed. Our state-of-art knowledge on the ages and characteristics of the IPS ophiolites is still too fragmentary to have a reliable data to propose any coherent hypothesis.

However, some important implications for the IP oceanic basin can be deduced from the data presented in this paper.

First, the data presented in this paper, as well those available (e.g., Göncüoğlu et al., 2008), indicate that the time span from middle Bathonian (Middle Jurassic) to early Tithonian (Late Jurassic) can be regarded as a period of active spreading in the IP oceanic basin.

Second, the new data from the Ayli Dağ ophiolites, i.e. an almost complete sequence representative of a back-arc type oceanic lithosphere and the geochemical data from the volcanics from the mélange of southern Armutlu Peninsula (e.g., Robertson and Ustaömer, 2004), even though from basalts of unknown age, indicate a subduction-related magmatism. All these data suggest that a subduction event in the

IP basin was progressed resulting in the back-arc basin development.

Third, the dominantly back-arc type Ayli Dağ ophiolites, characterized by IAT- and BABB-type volcanics, suggest that the oceanic lithosphere from IP oceanic basin started to be consumed before of the Middle Jurassic time by intra-oceanic subduction. This is coherent with the geochemical data obtained from the volcanic blocks within the Arkotdağ Mélange in Arac area (Catanzariti et al., 2012), indicating a wide range of tectonic settings that include mid-ocean ridge, plume-related or unrelated seamount/oceanic island as well as back-arc basin.

Ongoing study on the age of these volcanic rocks will certainly shed light on the evolution of the IP ocean basin.

CONCLUSIONS

The Ayli Dağ ophiolites, cropping out in the eastern part of the IPS zone in northern central Anatolia, are one of the largest occurrence of an almost complete ophiolitic sequence within the IPS zone. The geochemical evaluation of basalts from pillow-lavas and dykes suggests that the samples display subduction-related characteristics, similar to IAT- and BABB-type lavas generated in oceanic supra-subduction basin. While the very-depleted nature of the IAT-type samples can be explained by a mantle source that has experienced a previous melt extraction, MORB-like characteristics of the BABB-type samples are more suitable with a source similar to DMM.

The radiolarian cherts found at the top of the Ayli Dağ pillow lava sequence include characteristic taxa indicating to a depositional age of middle Bathonian to early Callovian.

The paleontological finding together with the tectono-magmatic evaluation suggest the presence of a Middle Jurassic back-arc spreading within the IP oceanic basin, which in turn indicates an intra-oceanic subduction during the same time interval. A review of previously published data of the authors shows that the IP oceanic basin between the SK and the IZ terranes had indeed a complex evolution.

Our new data place strong constraints for the existence of the IP oceanic basin that can be regarded as one of the Neotethys branches. However, to decipher the details of the evolution of the IP oceanic basin, more reliable data are required.

ACKNOWLEDGEMENTS

The authors gratefully acknowledge two anonymous reviewers. The research has been funded by Darius Project (resp. M. Marroni). This research benefits also by grants from PRIN 2008 project (resp. M. Marroni) and from IGG-CNR.

REFERENCES

- Aita Y., 1987. Middle Jurassic to Lower Cretaceous radiolarian biostratigraphy of Shikoku with reference to selected sections in Lombardy basin and Sicily. *Tohoku Univ., Sci. Reports*, 2nd ser. (Geology), 58 (1): 1-91.
- Akbayram K., Okay A.I. and Satir M., 2012. Early Cretaceous closure of the Intra-Pontide Ocean in western Pontides (northwestern Turkey). *J. Geodyn.*, in print. doi:10.1016/j.jog.2012.05.003.

- Arculus R.J., Lapierre H. and Jaillard E., 1999. Geochemical window into subduction and accretion processes: Raspas metamorphic complex, Ecuador. *Geology*, 27: 547-550.
- Baumgartner P. O., O'Dogherty L., Gorican S., Dumitrica-Jud R., Dumitrica P., Pillevuit A., Urquhart E., Matsuoka A., Danelian T., Bartolini A., Carter E.S., De Wever P., Kito N., Marcucci M. and Steiger T. 1995. Radiolarian catalogue and systematics of Middle Jurassic to Early Cretaceous Tethyan genera and species. In: P.O. Baumgartner et al. (Eds.), *Middle Jurassic to Lower Cretaceous Radiolaria of Tethys: occurrences, systematics, biochronology*. *Mém. Géol. (Lausanne)*, 23: 37-685.
- Beccaletto L., Bartolini A.C., Martini R., Hochuli P.A. and Kozur H., 2005. Biostratigraphic data from the Cetmi Mélange, north-west Turkey: Palaeogeographic and tectonic implications. *Palaeo. Palaeo. Palaeo.*, 221: 215-244.
- Bortolotti V. and Principi G., 2005. Tethyan ophiolites and Pangea break-up. *Island Arc*, 14: 442-470.
- Bortolotti V., Chiari M., Marcucci M., Photiades A., Principi G. and Saccani E., 2008. New geochemical and age data on the ophiolites from the Othrys area (Greece): Implication for the Triassic evolution of the Vardar Ocean. *Ofioliti*, 33: 135-151.
- Bortolotti V., Chiari M., Marroni M., Pandolfi L., Principi G. and Saccani E., 2012. Geodynamic evolution of ophiolites from Albania and Greece (Dinaric-Hellenic belt): one, two, or more oceanic basins? *Intern. J. of Earth Sci.*, doi: 10.1007/s00531-012-0835-7.
- Bozkurt E., Winchester J.A., Satir M., Crowley Q.G. and Ottley C.J., 2012. The Almacik mafic-ultramafic complex: exhumed Sakarya subcrustal mantle adjacent to the Istanbul Zone, NW Turkey, *Geol. Mag.*, doi: <http://dx.doi.org/10.1017/S0016756812000556>.
- Bragin N.Y., Tekin U.K. and Özçelik Y., 2002. Middle Jurassic Radiolarians from the Akgöl Formation, Central Pontides, northern Turkey. *N. J. Geol. Palaont. Monatsh.*, 10: 609-628.
- Catanzariti R., Ellero A., Göncüoğlu M.C., Marroni M., Ottria G. and Pandolfi L., 2012. Stratigraphical, paleontological and structural features of the Tarakli flysch in the Boyali Area: Evidences for the tectonic history of the Intra-Pontide suture zone. *65th Geol. Congr. Turkey, Abstr. Vol.*, p. 52-53.
- Chiari M., Bortolotti V., Marcucci M., Photiades A., Principi G. and Saccani E., 2012. Radiolarian biostratigraphy and geochemistry of the Koziakas Massif ophiolites. *Bull. Soc. géol. France*, 183 (4): 287-306.
- Chiari M., Djerić N., Garfagnoli F., Hrvatovic H., Krstić M., Levi N., Malasoma A., Marroni M., Menna F., Nirta G., Pandolfi L., Principi G., Saccani E., Stojadinović U. and Trivić B., 2011. The geology of the Zlatibor-Maljen area (western Serbia): a geotransverse across the ophiolites of the Dinaric-Hellenic collisional belt. *Ofioliti*, 36 (2): 137-164.
- Dumitrica P., 1970. *Cryptocephalic* and *Cryptothoracic Nasseleriain* in some Mesozoic deposits of Romania. *Rev. Roumaine Géol., Géophys. Géogr., Sér. Géol.*, 14 (1): 45-124.
- Ellam R.M. and Hawkesworth C.J., 1988. Elemental and isotopic variations in subduction related basalts: evidence for a three component model. *Contrib. Mineral. Petrol.*, 98: 72-80.
- Elliott T., Plank T., Zindler A., White W. and Bourdon B., 1997. Element transport from slab to volcanic front at the Mariana arc. *J. Geophys. Res.*, 102: 14991-15019.
- Elmas A. and Yigitbas E., 2001. Ophiolite emplacement by strike-slip tectonics between the Pontide Zone and the Sakarya Zone in northwestern Anatolia, Turkey. *Int. J. Earth Sci.*, 90: 257-269.
- Elmas A. and Yigitbas E., 2005. Comment on "Tectonic evolution of the Intra-Pontide suture zone in the Armutlu Peninsula, NW Turkey" by Robertson and Ustaömer. *Tectonophysics*, 405: 213-221.
- Elmas A., 2012. Basement types of the Thrace Basin and a new approach to the pre-Eocene tectonic evolution of the northeastern Aegean and northwestern Anatolia: a review of data and concepts. *Int. J. Earth Sci.*, 101, 1895-1911. DOI 10.1007/s00531-012-0756-5
- Elmas A., Yigitbas E. and Yılmaz Y., 1997. The geology of the Bolu - Eskipazar zone: an approach to the development of the Intra-Pontide Suture. *Geosound*, 30: 1-14.
- Fretzdorff S., Livermore R.A., Devey C.W., Leat P.T. and Stoffers P., 2002. Petrogenesis of the Back-arc East Scotia Ridge, South Atlantic Ocean. *J. Petrol.*, 43: 1435-1467.
- Göncüoğlu M.C. and Erendil M., 1990. Pre-Late Cretaceous tectonic units of the Armutlu Peninsula. *Proceed. 8th Turk. Petrol. Congr.*, 8: 161-168.
- Göncüoğlu M.C., Dirik K. and Kozlu H., 1997. General characteristics of pre-Alpine and Alpine terranes in Turkey: Explanatory notes to the terrane map of Turkey. *Ann. Géol. Pays Hellén., Geol. Soc. Greece*, 37: 515-536.
- Göncüoğlu M.C., Erendil M., Tekeli O., Aksay A., Kuscu A. and Ürgün B., 1987. Geology of the Armutlu Peninsula. *IGCP-5 Guide Book for the field excursion along Western Anatolia, Turkey, Ankara*, 5: 12-18.
- Göncüoğlu M.C., Gürsü S., Tekin U.K. and Köksal S., 2008. New data on the evolution of the Neotethyan oceanic branches in Turkey: Late Jurassic ridge spreading in the Intra-Pontide branch. *Ofioliti*, 33: 153-164.
- Gribble R.F., Stern R.J., Bloomer S.H., Stuben D., O'Hearn T. and Newman S., 1996. MORB mantle and subduction components interact to generate basalts in the southern Mariana Trough back-arc basin. *Geochim. Cosmochim. Acta*, 60: 2153-2166.
- Gribble R.F., Stern R.J., Newman S., Bloomer S.H. and O'Hearn T., 1998. Chemical and isotopic composition of lavas from the northern Mariana Trough; implications for magma genesis in back-arc basins. *J. Petrol.*, 39: 125-154.
- Hawkins J.W. and Evans C.E., 1983. Geology of the Zambales Range, Luzon, Philippine Islands: ophiolite derived from an island arc-back-arc pair. In: D.E. Hayes (Ed.), *The tectonics and geologic evolution of southeast Asian seas and islands, Part 2*. *AGU Geophys. Monogr.*, 27: 124-138.
- Ichiyama Y. and Ishiwatari A., 2004. Petrochemical evidence for off-ridge magmatism in a back-arc setting from the Yakuno ophiolite, Japan. *Island Arc*, 13: 157-177.
- Kaya O. and Kozur H., 1987. A new and different Jurassic to Early Cretaceous sedimentary assemblage in northwestern Turkey (Gemlik, Bursa): implications for the pre-Jurassic to Early Cretaceous tectonic evolution. *Yerbilimleri*, 14: 253-268.
- Kozur H.W., Aydın M., Demir O., Yakar H., Göncüoğlu M.C. and Kuru F., 2000. New stratigraphic results from the Paleozoic and Early Mesozoic of the Middle Pontides (northern Turkey) in the Azdavay, Devrekani, Küre and Inebolu areas: implications for the Carboniferous-Early Cretaceous geodynamic evolution and some related remarks to the Karakaya oceanic rift basin. *Geol. Croatica*, 53: 209-268
- Leat P.T., Pearce J.A., Barker P.F., Millar I.L., Barry T.L. and Larter R.D., 2004. Magma genesis and mantle flow at a subducting slab edge: the South Sandwich arc-basin system. *Earth Planet. Sci. Lett.*, 227: 17-35.
- Lissenberg C.J., van Staal C.R., Bedard J.H. and Zagorevski A., 2005. Geochemical constraints on the origin of the Annieopsquotch ophiolite belt, southwest Newfoundland. *Geol. Soc. Am. Bull.*, 117: 1413-1426.
- Ludden J., Gelin L. and Trudel P., 1982. Archean metavolcanics from the Rouyn-Noranda district, Abitibi Greenstone Belt, Quebec. 2. Mobility of trace elements and petrogenetic constraints. *Can. J. Earth Sci.*, 19: 2276-2287.
- McCulloch M.T. and Gamble J.A., 1991. Geochemical and geodynamical constraints on subduction zone magmatism. *Earth Planet. Sci. Lett.* 102: 358-374.
- McKenzie D. and O'Nions R.K., 1991. Partial melt distributions from inversion of rare earth element concentrations. *J. Petrol.*, 32: 1021-1091.
- Moix P., Beccaletto L., Kozur H.W., Hochard C., Rosselet F. and Stampfli G.M., 2008. A new classification of the Turkish terranes and sutures and its implication for the paleotectonic history of the region. *Tectonophysics*, 451: 7-39.

- Nagai H. and Mizutani S., 1990. Jurassic *Eucyrtidellium* (radiolaria) in the Mino Terrane. *Trans. Proc. Paleont. Soc. Japan, N. S.*, 159: 587-602.
- Okay A.I. and Tüysüz O., 1999. Tethyan sutures of northern Turkey. In: B. Durand, J.L. Olivet, E. Horvath and M. Serrane (Eds.), *The Mediterranean basins, extension within the Alpine Orogen*. *Geol. Soc. London Spec. Publ.*, 156: 475-515.
- Okay A.I. and Whitney D.L., 2010. Blueschists, eclogites, ophiolites and suture zones in northwest Turkey: a review and a field excursion guide. *Ofioliti*, 35 (2): 131-172.
- Ozoldava L., 1975. Upper Jurassic radiolarians from the Kysuca series in the Klippen Belt. *Zapad. Karp., Seria Paleont.*, 1: 73-86.
- Ozoldova L., 1998. Middle Jurassic Radiolarian assemblages from Radiolarites of the Silica nappe (Slovak karst, western Carpathians). *Geol. Carpat.*, 49 (4): 289-296.
- Pearce J.A. and Parkinson I.J., 1993. Trace element models for mantle melting: application to volcanic arc petrogenesis. In: H.M. Prichard, T. Alabaster, N.B.W. Harris and C.R. Neary (Eds.), *Magmatic processes and plate tectonics*. *Geol. Soc. London Spec. Publ.*, 76: 373-403.
- Pearce J.A. and Peate D.W., 1995. Tectonic implications of the composition of volcanic arc magmas. *Ann. Rev. Earth Planet Sci.*, 23: 251-285.
- Pearce J.A., 1983. The role of sub-continental lithosphere in magma genesis at active continental margins. In: C.J. Hawkesworth and M.J. Norry (Eds.), *Continental basalts and mantle xenoliths*, Nantwich (Shiva Publ.), p. 230-249.
- Pearce J.A., Baker P.E., Harvey P.K. and Luff I.W., 1995. Geochemical evidence for subduction fluxes, mantle melting and fractional crystallization beneath the South Sandwich Island Arc. *J. Petrol.*, 36: 1073-1109.
- Pearce J.A., 1996. A users guide to basalt discrimination diagrams. In: D.A. Wyman (Ed.), *Trace Element geochemistry of volcanic rocks: Applications for massive sulphide exploration*. *Geol. Ass. Can., Short Course Notes*, 12: 79-113.
- Peate D.W., Pearce J.A., Hawkesworth C.J., Colley H., Edwards C.M.H. and Hirose K., 1997. Geochemical variations in Vanuatu arc lavas: the role of subducted material and a variable mantle wedge composition. *J. Petrol.*, 38: 1331-1358.
- Pessagno E.A.Jr., Blome C.D., Mayerhoff Hull D. and Six W.M., 1993. Jurassic radiolaria from the Josephine ophiolite and overlying strata, Smith River subterranean (Klamath Mountains), northwestern California and southwestern Oregon. *Micropal.*, 39 (2): 93-166.
- Pessagno E.A.Jr. and Newport R.L., 1972. A new technique for extracting radiolaria from radiolarian cherts. *Micropal.*, 18 (2): 231-234.
- Pessagno E.A.Jr., 1977. Upper Jurassic Radiolaria and radiolarian biostratigraphy of the California Coast Ranges. *Micropal.*, 23 (1): 56-113.
- Robertson A.H.F., 2002. Overview of the genesis and emplacement of Mesozoic ophiolites in the Eastern Mediterranean Tethyan region. *Lithos*, 65: 1-67.
- Robertson A.H.F., Clift P.D., Degnan P.J. and Jones G., 1991. Palaeogeographical and palaeotectonic evolution of the eastern Mediterranean Neotethys. *Palaeogeogr. Palaeoclim. Palaeoecol.*, 87: 289-343.
- Robertson A.H.F. and Dixon J.E. 1984. Introduction: aspects of the geological evolution of the Eastern Mediterranean. In: J.E. Dixon and A.H.F. Robertson (Eds.), *The geological evolution of the Eastern Mediterranean*. *Geol. Soc. London Spec. Publ.* 17: 1-73.
- Robertson A.H.F. and Ustaömer T., 2004. Tectonic evolution of the Intra-Pontide suture zone in the Armutlu Peninsula, NW Turkey. *Tectonophysics*, 381: 175-209.
- Saccani E., Bortolotti V., Marroni M., Pandolfi L., Photiades A. and Principi G., 2008c. The Jurassic association of backarc basin ophiolites and calc-alkaline volcanics in the Guevgueli Complex (northern Greece): Implication for the evolution of the Vardar Zone. *Ofioliti*, 33: 209-227.
- Saccani E., Photiades A. and Beccaluva L., 2008a. Petrogenesis and tectonic significance of IAT magma-types in the Hellenide ophiolites as deduced from the Rhodiani ophiolites (Pelagonian zone, Greece). *Lithos*, 104: 71-84.
- Saccani E., Photiades A., Santato A. and Zeda O., 2008b. New evidence for supra-subduction zone ophiolites in the Vardar zone from the Vermion massif (northern Greece): Implication for the tectono-magmatic evolution of the Vardar oceanic basin. *Ofioliti*, 33: 65-85.
- Schmid S.M., Bernoulli D., Fügenschuh B., Matenco L., Schefer S., Schuster R., Tischler M. and Ustaszewski K., 2008. The Alpine-Carpathian-Dinaridic orogenic system: correlation and evolution of tectonic Units. *Swiss. J. Geosci.*, 101: 139-183.
- Sengör A.M.C., 1986. The dual nature of the Alpine-Himalayan system: Progress, problems and prospects. *Tectonophysics*, 127: 177-195.
- Sengör A.M.C. and Yılmaz Y., 1981. Tethyan evolution of Turkey: a plate tectonic approach. *Tectonophysics*, 75: 181-241.
- Shervais M., 1982. Ti-V plots and the petrogenesis of modern and ophiolitic lavas. *Earth Planet. Sci. Lett.*, 59: 101-118.
- Sinton J.M., Ford L.L., Chappell B. and McCulloch M.T., 2003. Magma genesis and mantle heterogeneity in the Manus Back-Arc Basin, Papua New Guinea. *J. Petrol.*, 44: 159-195.
- Stampfli G.N., 2000. Tethyan Oceans. In: E. Bozkurt, J. Winchester and J.A. Piper, (Eds.), *Tectonics and magmatism in Turkey and the surrounding area*. *Geol. Soc. London Spec. Publ.*, 173: 1-23.
- Staudigel H., Plank T., White B. and Schmincke H-U., 1996. Geochemical fluxes during seafloor alteration of the basaltic upper oceanic crust: DSDP sites 417 and 418. *Geophys. Monogr. Ser.*, 96: 19-38.
- Sun S.-S. and McDonough W.F., 1989. Chemical and isotopic systematics of oceanic basalts: implications for mantle composition and processes. In: A.D. Saunders and M.J. Norry (Eds.), *Magmatism in the ocean basins*. *Geol. Soc. London Spec. Publ.*, 42: 313-345.
- Tekin U.K. and Göncüoğlu M.C., 2009. Late Middle Jurassic (Late Bathonian-Early Callovian) radiolarian cherts from the Neotethyan Bornova Flysch Zone, Spil Mountains, Western Turkey. *Stratig. Geol. Correl.*, 17 (3): 298-308.
- Tokay M., 1973. Geological observations on them North Anatolian Fault Zone between Gerede and Ilgaz. *Proceed. North Anatolian Fault and Earthquakes Symp.*, M.T.A. Publ., p. 12-29.
- Tollan P.M.E., Bindeman I. and Blundy J.D., 2011. Cumulate xenoliths from St. Vincent, Lesser Antilles Island Arc: a window into upper crustal differentiation of mantle-derived basalts. *Contrib. Mineral. Petrol.*, 163: 189-208.
- Tüysüz O. and Tekin U.K., 2007. Timing of imbrication of an active continental margin facing the northern branch of Neotethys, Kargi Massif, northern Turkey. *Cret. Res.*, 28 (3): 754-764.
- Varol E., Bedi Y., Tekin U.K. and Uzuncimen S., 2011. Geochemical and petrological characteristics of Late Triassic basic volcanic rocks from the Kocali complex, SE Turkey: implications for the Triassic evolution of southern Tethys. *Ofioliti*, 36 (1): 101-115.
- Ulgen S.C. and Okay A.I. 2010. Tectonic setting of the ophiolitic mélanges south of the Marmara Sea between the Izmir-Ankara and Intra-Pontide sutures. *Tectonic Crossroads: Evolving Orogens of Eurasia-Africa-Arabia*, GSA-Meeting, Ankara, Abstr., Nr. 27.
- Winchester J.A. and Floyd P.A., 1977. Geochemical discrimination of different magma series and their differentiation products using immobile elements. *Chem. Geol.*, 20: 325-343.
- Woodhead J., Eggins S. and Gamble J., 1993. High field strength and transition element systematics in island arc and back-arc basin basalts: evidence for multi-phase melt extraction and a depleted mantle wedge. *Earth Planet. Sci. Lett.*, 114: 491-504.
- Woodhead J.D., Eggins S.M. and Johnson R.W., 1998. Magma genesis in the New Britain island arc: further insights into melting and mass transfer processes. *J. Petrol.*, 39: 1641-1668.

- Workman R.K. and Hart S.R., 2005. Major and trace element composition of the depleted MORB mantle (DMM). *Earth Planet. Sci. Lett.*, 231: 53-72.
- Yigitbas E., Elmas A, and Yılmaz Y., 1999. Pre-Cenozoic tectonostratigraphic components of the Western Pontides and their geological evolution. *Geol. J.*, 34: 55-74.
- Yılmaz Y., Gözübol A.M. and Tüysüz O., 1982. Geology of an area in and around the Northern Anatolian transform Fault Zone between Bolu and Akyaz. In: A.M. Iskara and A. Vogel (Eds.), *Multidisciplinary approach to earthquake prediction*. Friedr. Vieweg and Sohn, Braunsch., p. 45-65.
- Zelic M., Marroni M., Pandolfi L. and Trivic B., 2010. Tectonic setting of the Vardar suture zone (Dinaric-Hellenic belt): the example of the Kopaonik area (southern Serbia). *Ofioliti*, 35 (1): 49-69.
- Zindler A. and Hart S., 1986. Chemical geodynamics. *Ann. Rev. Earth Planet. Sci.*, 14: 493-571.

Received, September 5, 2012
Accepted, December 10, 2012

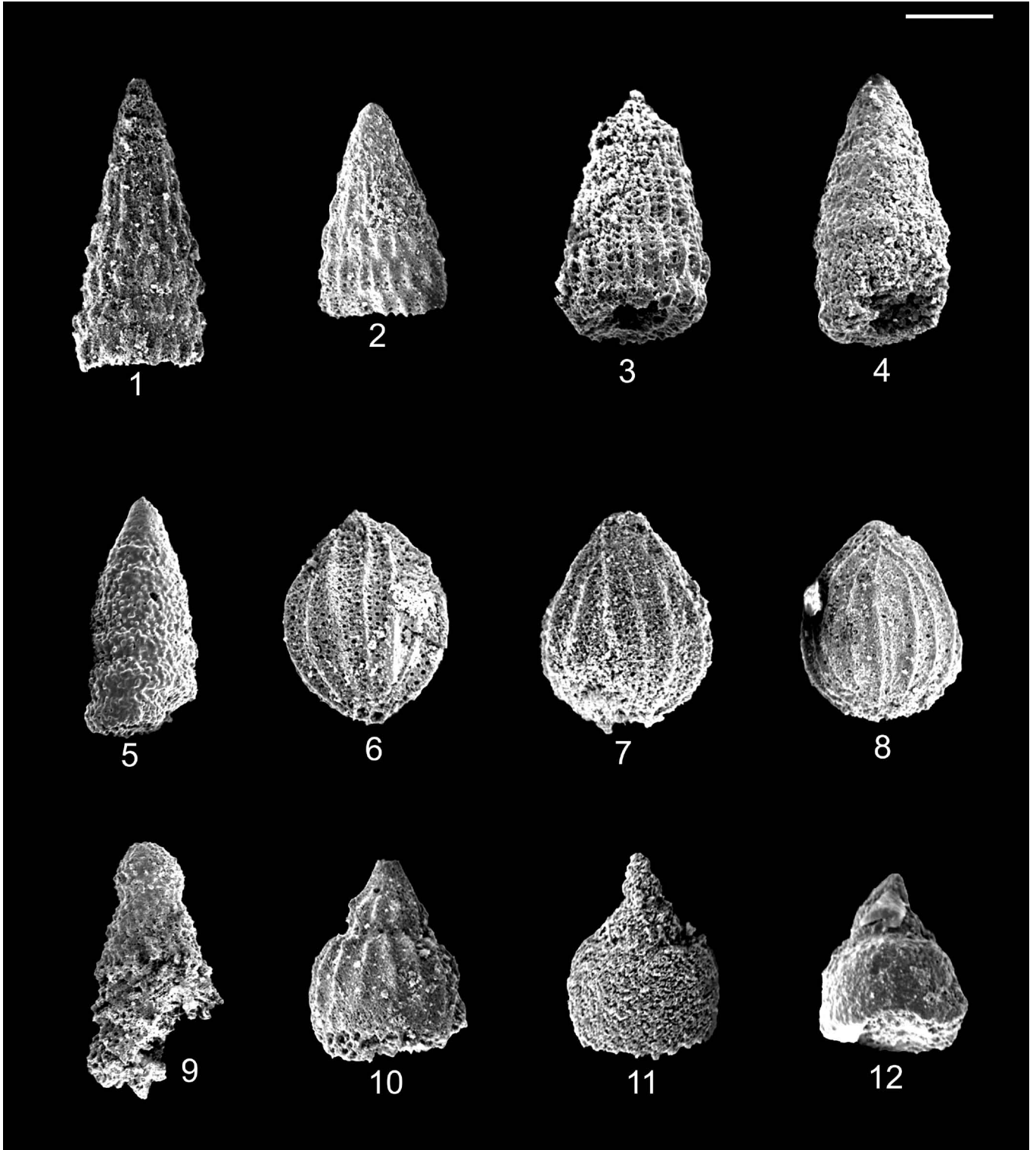


Plate 1 - Scanning electron micrographs of the middle Bathonian to early Callovian radiolarians from the Ayli Dağ ophiolites, northern Turkey. Scale- number of microns for each figure. 1) *Transsuum brevicostatum* gr. (Ozoldova), sample no. 11-TC-108, scale bar- 70µm; 2) *Transsuum* sp. cf. *T. brevicostatum* gr. (Ozoldova), sample no. 11-TC-109, scale bar- 70µm; 3) *Transsuum* sp. aff. *T. maxwelli* gr. (Pessagno), sample no. 11-TC-109, scale bar- 60µm; 4-5) *Spongocapsula palmerae* Pessagno; 4) sample no. 11-TC-108; 5) sample no. 11-TC-109, scale bar for both specimens- 80µm; 6-8) *Unuma gordus* Hull, 6-7- sample no. 11-TC-108, 8- sample no. 11-TC-109, scale bar for all specimens- 60µm; 9) *Stichomitra* (?) *takanoensis* Aita, sample no. 11-TC-109, scale bar- 70µm; 10) *Eucyrtidiellum semifactum* Nagai and Mizutani, sample no. 11-TC-108, scale bar- 60µm; 11) *Eucyrtidiellum* sp., sample no. 11-TC-108, scale bar- 40µm; 12) *Eucyrtidiellum unumaense pustulatum* Baumgartner, sample no. 11-TC-109, scale bar- 40µm.